Published in final edited form as:
Biochemistry. 2009 October 27; 48(42): 10183–10191. doi:10.1021/bi901429y.

Expressed Phosphorylase *b* Kinase and Its α*γδ* Subcomplex as Regulatory Models for the Rabbit Skeletal Muscle Holoenzyme†

Igor G. Boulatnikov[‡], **Jennifer L. Peters**[‡], **Owen W. Nadeau**[‡], **Jessica M. Sage**[‡], **Patrick J. Daniels**[‡,§], **Priyadarsini Kumar**[||], **Donal A. Walsh**[⊥], and **Gerald M. Carlson**[‡,*]

[‡]Department of Biochemistry and Molecular Biology, University of Kansas Medical Center, Kansas City, Kansas 66160

[||]Department of Cell Biology and Human Anatomy, University of California, Davis, California 95616

[⊥]Department of Medicine and Epidemiology, School of Veterinary Medicine, University of California, Davis, California 95616

Abstract

Understanding the regulatory interactions among the 16 subunits of the $(\alpha\beta\gamma\delta)_4$ phosphorylase *b* kinase (PhK) complex can only be achieved through reconstructing the holoenzyme or its subcomplexes from the individual subunits. In this study, recombinant baculovirus carrying a vector containing a multigene cassette was created to coexpress in insect cells α, *β*, *γ*, and *δ* subunits corresponding to rabbit skeletal muscle PhK. The hexadecameric recombinant PhK (rPhK) and its corresponding $\alpha\gamma\delta$ trimeric subcomplex were purified to homogeneity with proper subunit stoichiometries. The catalytic activity of rPhK at pH 8.2 and its ratio of activities at pH 6.8 versus pH 8.2 were comparable to those of PhK purified from rabbit muscle (RM PhK), as was the hysteresis (autoactivation) in the rate of product formation at pH 6.8. Both the rPhK and $\alpha\gamma\delta$ exhibited only a very low Ca^{2+}-independent activity and a Ca^{2+}-dependent activity similar to that of the native holoenzyme with $[Ca^{2+}]_{0.5}$ of 0.4 μM for the RM PhK, 0.7 μM for the rPhK, and 1.5 μM for the $\alpha\gamma\delta$ trimer. The RM PhK, rPhK, and $\alpha\gamma\delta$ subcomplex were also all activated through self-phosphorylation. Using cross-linking and limited proteolysis, the α–*γ* intersubunit contacts previously observed within the intact RM PhK complex were also observed within the recombinant $\alpha\gamma\delta$ subcomplex. Our results indicate that both the rPhK and $\alpha\gamma\delta$ subcomplex are promising models for future structure–function studies on the regulation of PhK activity through intersubunit contacts, because both retained the regulatory properties of the enzyme purified from skeletal muscle.

Phosphorylase *b* kinase (PhK),[1] a hexadecameric enzyme complex with $(\alpha\beta\gamma\delta)_4$ subunit stoichiometry (1), controls glycogen degradation via phosphorylation of glycogen

†This work was supported by U.S. Public Health Service Grant DK32953.

*Corresponding author: gcarlson@kumc.edu; telephone, 913-588-7108; fax, 913-588-7005.
§Current address: Math and Science Department, Corban College, 5000 Deer Park Drive SE, Salem, OR 97317

SUPPORTING INFORMATION AVAILABLE

Themethod for the polymerase chain reaction, construction of transfer vectors and preparation of recombinant baculoviruses (rBV), and the generation of the rBV for PhK. This material is available free of charge via the Internet at http://pubs.acs.org.

[1]Abbreviations: PhK, phosphorylase *b* kinase; GP*b*, glycogen phosphorylase *b*; CaM, calmodulin; RM PhK, phosphorylase *b* kinase purified from rabbit skeletal muscle; rPhK, recombinant baculovirus-expressed rabbit muscle phosphorylase *b* kinase; BAPTA, 1,2-bis(*o*-aminophenoxy) ethane-*N*,*N*,*N*′,*N*′-tetraacetic acid; rBV, recombinant baculovirus; MCS, multiple cloning site; KUMC, University of Kansas Medical Center; *γ*CRD, C-terminal regulatory domain of the *γ* subunit.

phosphorylase *b* (GP*b*). The kinase activity, which resides on the catalytic γ subunit, has an obligatory requirement for Ca^{2+}, which binds to PhK's intrinsic calmodulin (CaM) subunit, δ, and couples muscle contraction with energy production via glycogenolysis (2). In addition to Ca^{2+}, a large number of other activators further enhance PhK's activity at neutral pH, mostly by binding to allosteric sites on its large, regulatory α and β subunits (2). Phosphorylation of the α and particularly β subunits also markedly stimulates PhK activity at neutral pH (3). Thus the PhK complex has evolved the capacity to have its activity regulated by a diverse group of activators; in fact, summing the masses of its regulatory α (138.4 kDa (4, 5)), β (125.2 kDa (5)), and δ (16.7 kDa (6)) subunits and the C-terminal regulatory domain of its catalytic γ subunit (11.7 of 44.7 kDa (7)), one finds that a full 90% of PhK's 1.3 MDa mass is noncatalytic, presumably largely devoted to its regulation.

The mechanisms through which the diverse allosteric activators acting on the α, β, and δ regulatory subunits stimulate the activity of the catalytic γ subunit of PhK remains for the most part unknown, in large part because structure–function studies using mutagenesis to probe the regulation of the PhK complex have not been feasible. A critical breakthrough in this regard was made 5 years ago with the first reported expression, utilizing baculovirus, of the PhK holoenzyme complex, as well as its αγδ and γδ subcomplexes (8). For practical reasons, that study used separate vectors for each of the four subunits, with α, γ, and δ from rat and β from rabbit. Importantly, the coexpressed subunits of the PhK holoenzyme did assemble in the appropriate subunit stoichiometry and exhibit pH- and Ca^{2+}-dependent activities that were similar to those of PhK purified from fast-twitch skeletal muscle of the rabbit (RM PhK), which is the form of the enzyme for which virtually all reference information has been obtained during the last 55 years (2). There were, however, some key differences between the properties of the expressed recombinant PhK (rPhK) and RM PhK: specific activity at pH 8.2 (25%of that expected); high Ca^{2+}-independent basal activity (50%); K_a for Ca^{2+} (one-tenth the normal required concentration); no activation upon phosphorylation of the α and β subunits; and pH 6.8/8.2 activity ratio (0.40 instead of<0.05). This last property is significant because the ratio of activities at these two pH values is an accepted indicator of the activation state of wt PhK (9). So, although this first expression system represented a huge step forward and proved the feasibility of producing active, hexadecameric rPhK, the resultant PhK complex was not yet suitable for structure–function studies aimed at understanding the control of PhK activity by its regulatory subunits.

In the work herein, we set about improving the previous system, with the goal of producing rPhK having properties that closely mimic those of isolated rabbit skeletal muscle PhK. We focused on three major changes to the published expression system. First, we chose to use cDNA from rabbit for the α, β, and γ subunits. Even though the sequences for the various subunits are highly conserved between rabbit and rat (2), we reasoned that even small differences might affect subunit interactions and regulatory properties. The cDNA used for CaM, the δ subunit, was from *Xenopus* and codes for CaM with a sequence identical to that of rabbit (10, 11). Second, to allow stoichiometric expression of the four subunits that could be reproducibly maintained, we desired that all four subunits be expressed by a single vector, rather than four as in the published procedure. Third, we decided that when a His_6 tag was used, it would be placed on a different subunit than the catalytic γ, as was done previously. We opted for the N-terminus of the α subunit, in that this region has yet to be implicated in any property of PhK. As is described herein, we have effected these three changes and produced a rPhK complex with properties that very closely mimic those of PhK isolated from muscle, thus allowing future structure–function studies on the intersubunit regulation of PhK activity.

EXPERIMENTAL PROCEDURES

Materials and Reagents

TA cloning kits, Ni-NTA agarose, HisPur cCobalt resin (Co^{2+}-agarose-6B CL), Cellfectin reagent, and BAPTA were from Invitrogen Co. (Carlsbad, CA). QIA-quick PCR purification and gel extraction kits were from Qiagen (Valencia, CA). Oligonucleotide primers were synthesized by Integrated DNA Technologies (Coralville, IA). [γ-^{32}P]ATP was from Perkin-Elmer Life Sciences, Inc. (Boston, MA). Fura-2 fluorescent dye was from Calbiochem (San Diego, CA). Paraformaldehyde, iodoacetamide, Sephacryl S-300 HR, and all protease inhibitors were from Sigma Chemical Co. (St. Louis, MO). TSK gel Toyopearl HW-55F was from Toyo Soda Mfg. Co., Ltd. (Tokyo, Japan); all other chromatography resins were from Amersham Biosciences (Piscataway, NJ). Reagents, materials, and molecular weight standards for SDS–PAGE were from Bio-Rad Laboratories (Hercules, CA). The formaldehyde cross-linker was prepared by the hydrolysis of paraformaldehyde (12).

Proteins and Enzymes

Platinum Taq DNA polymerase high fidelity was from Invitrogen, and DNA restriction enzymes and T4 ligase were from New England Biolabs (Beverly, MA). Chymotrypsin was from Worthington Biochemical Co. (Freehold, NJ). Anti-PhK α, β, and γ subunit-specific monoclonal antibodies (mAbs) were produced in mice using PhK as antigen (13, 14). The anti-CaM mAb (clone CaM85) was from Zymed Laboratories, Inc. (South San Francisco, CA). Guinea pig polyclonal antibodies (pAbs) against the α, β, and γ subunits of PhK were described previously (8). The penta-His mouse mAb was from S Prime Inc. (Gaithersburg, MD). Alkaline phosphatase detection conjugates were from Southern Biotechnology (Birmingham, AL). GP*b* was isolated from rabbit skeletal muscle (15), and residual AMP was removed with charcoal. Rabbit muscle PhK was purified from psoas muscle of New Zealand White rabbits as described previously (16). The concentrations of GP*b* and wt PhK were determined spectrophotometrically using absorbance indexes of 13.0 (17) and 12.4 (18), respectively, for 1% solutions at 280 nm. Recombinant $(\alpha\beta\gamma\delta)_4$ PhK and the $\alpha\gamma\delta$ subcomplex were isolated and purified as described below. Concentrations of purified rPhK and $\alpha\gamma\delta$ were determined by the Pierce BCA assay (Thermoscientific, Rockford, IL) using the provided albumin standard. Subunits of the recombinant $(\alpha\beta\gamma\delta)_4$ and $\alpha\gamma\delta$ complexes were identified on the basis of their apparent mass and cross-reactivity with mAbs against the subunits of PhK. Relative amounts of the α, β, and γ subunits in preparations of rPhK and $\alpha\gamma\delta$ were determined by measuring their optical densities in Coomassie-stained gels. Gel densitometry was performed using a Fluorochem 8900 analyzer (Alpha Innotech, San Leandro, CA).

Cell Culture

Sf9 and Hi-5 insect cells [gift of Dr. Gustavo Blanco, University of Kansas Medical Center (KUMC)] were maintained in monolayer cultures at 27 °C in BD-Baculogold TNM-FH media (BD Pharmingen, San Jose, CA) and EX-CELL 405 serum-free media with L-Gln (SAFC Biosciences, Lenexa, KS), respectively. Each was supplemented with penicillin and streptomycin (Cellgro Mediatech, Manassas, VA).

Purification of Recombinant PhK Complexes

In the purification of His_6-$\alpha\gamma\delta$, Hi-5 cells were seeded into 150 mm cell culture dishes and incubated at 27 °C either for 40 h or until cells reached 60% confluence. The cells were subsequently infected with a single rBV bearing the α, γ, and δ subunits of rabbit muscle PhK in EX-CELL 405media using a multiplicity of infection of 5. At 60 h postinfection, the

cells were lysed and the His_6-α$\gamma\delta$ subcomplex was purified, essentially as described (8), but with additional protease inhibitors (10 μg/mL N_α-*p*-tosyl-L-arginine methyl ester and 1 μg/mL *N*-α-benzoyl-L-arginine methyl ester) included in the cell lysis buffer. The purity of the complex after each chromatographic step was assessed by SDS–PAGE on 6–18%linear polyacrylamide gels stained with Coomassie Brilliant Blue R-250 and Bismarck Brown R (19). Subunits were identified by their apparent mass and cross-reactivity against mAbs specific for the subunits of PhK and the His_6 tag on α. PurifiedHis_6-α$\gamma\delta$ (typically 4–8 mg/mL) was stored (short-term) in small aliquots in 50 mM Hepes (pH 6.8), 5% sucrose, 0.1 mM EDTA, and 14 mM β-mercaptoethanol at −20 °C. For a long-term storage, glycerol was added to a final concentration of 50%. Prior to carrying out assays or experiments with the α$\gamma\delta$ complex, glycerol was removed by ultrafiltration with 10 kDa MWCO Centricon filters (Millipore, Billerica, MA).

For purification of His_6-rPhK, Hi-5 cells were treated as described above for His_6-α$\gamma\delta$. The cells were then infected with a single rBV expressing the α, β, γ, and δ subunits of rabbit muscle PhK in EX-CELL 405 media using a multiplicity of infection of 5. Sixty-five hours postinfection, the cells were scraped from the dishes using ice-cold PBS and harvested by centrifugation at 800*g* for 10 min at 7 °C. The resulting cell pellet was resuspended in ice-cooled buffer A [50 mM β-glycerophosphate (pH6.8), 10%sucrose, 10mMNaCl, 2mM benzamidine, 1 mM 4-(2-aminoethyl)benzenesulfonyl fluoride hydrochloride, 0.1 mM *N*-*p*-tosyl-L-phenylalanine chloromethyl ketone, 0.05 mM N_α-*p*-tosyl-L-lysine chloromethyl ketone, 2.3 μM leupeptin, 1.4 μM pepstatin A, 0.15 μM aprotinin, 2.8 μM E-64], followed by a 10min equilibration at 300 psi in a ParrN_2 cavitation bomb cooled on ice. The cells were then lysed by extrusion from the bomb. The resulting crude homogenate was centrifuged at 4 °C for 30min at 10000*g* to recover the cytosolic protein fraction. The clarified lysate was loaded onto a Co^{2+}-agarose-6B CL column equilibrated in buffer B [50 mM sodium phosphate (pH 7.4), 300 mM NaCl, 10% glycerol, 5% sucrose, 2 mM benzamidine hydrochloride, and 10 mM imidazole]. After rinsing with 10 column volumes of buffer B and an additional 10 column volumes with buffer B containing 20 mM imidazole, bound protein was eluted with 150 mM imidazole in buffer B. Fractions (0.5 mL each) were collected and analyzed for protein content. Those containing high concentrations of protein were pooled and loaded onto a 1.4 cm × 75 cm Sephacryl S-300HR column (flow rate of 10 mL/h) that had been equilibrated in buffer C [50 mM Hepes (pH 6.8), 0.1 mM EDTA, 5%sucrose, 50 mM NaCl, and 14 mM β-mercaptoethanol]. The eluate was fractionated (1 mL) and monitored for protein content by absorbance (280 nm). Protein-containing fractions with retention times corresponding to RM PhK were pooled and dialyzed overnight against buffer D [50mMHepes (pH 6.8), 5%sucrose, 0.1mMEDTA, and 14mM β-mercaptoethanol], concentrated to 2 mg/mL with Amicon Ultra 100 kDa molecular weight cutoff filters (Millipore, Billerica, MA), analyzed by Western blot analyses as described above for α$\gamma\delta$, and stored at −20 °C.

GPb Conversion Assay

PhK activity was measured using a phosphocellulose P81 (Whatman, Rockland, MA) paper assay (20), with minor modifications (21). Incorporation of phosphate into GP*b* by rPhK and its α$\gamma\delta$ subcomplex was determined as recently reported (22).

Ca^{2+}-Dependent Activation of the PhK $(\alpha\beta\gamma\delta)_4$ and αγδ Complexes

GP*b* conversion assays were carried out for RM PhK (0.9 nM), rPhK (0.9 nM), and α$\gamma\delta$ (3.5 nM) in reaction buffers containing 50 mM Tris/53 mM β-glycerophosphate (pH 8.2), 10 mM $Mg(CH_3CO_2)_2$, 4.05 mM BAPTA, 8 μM EGTA, 2.24 mM β-mercaptoethanol, 1.5 mM [γ-^{32}P]ATP (480 Ci/mol), and 12 μM GP*b*. The concentrations of ATP and BAPTA (23) were determined spectrophotometrically using their respective molar extinction coefficients:

$\varepsilon_{\lambda 259nm}$ 15400 (pH 7.0) and $\varepsilon_{\lambda 287nm}$ 5600. Free Ca^{2+} concentrations ($[Ca^{2+}]_{free}$: 0.0155, 0.0353, 0.0866, 0.595, 2.08, 2.85, 3.47, 5.50, and 28.48 μM) were determined experimentally by carrying out fluorescence measurements of solutions containing 5 μMFura-2 indicator (24) and all the components of the reaction mixture listed above except GP*b*, which interfered with fluorescence measurements using the Fura-2 probe. GP*b* additions were substituted by adding equivalent volumes of GP*b* carrier buffer. Measurements were conducted in quartz cells (Starna Cells, Inc., Atascadero, CA) at 30 °C using either a Spex Fluorolog 322 or PTI spectrofluorometer, with a slit width adjustment of 2 nm for both the excitation (340 and 380 nm) and emission (510 nm) wavelengths. Fluorescence intensity (F) measurements were used to calculate final $[Ca^{2+}]_{free}$ values using the equation $[Ca^{2+}]_{free}=K_d\beta(R_i - R_{min})/(R_{max} - R_i)$ (25), where K_d is the apparent dissociation constant (135 nM) determined for the [fura-2–Ca^{2+}] complex (26) and R_i is the background corrected fluorescence (F_{340}/F_{380}). All other components of the equation (β = F_{380} at zero Ca^{2+}/F_{380} at saturated Ca^{2+}; $R_{min}=F_{340}/F_{380}$ at zero Ca^{2+}; and $R_{max}=F_{340}/F_{380}$ at saturated Ca^{2+}) were determined experimentally as previously described (27).

Autophosphorylation Assay

Phosphate incorporation into the regulatory β and/or α subunits of RM PhK, rPhK, and $\alpha\gamma\delta$ was carried out essentially as reported (8), with the following modifications. Final concentrations of each component in the autophosphorylation reaction were 67 mMβ-glycerophosphate/50 mM Tris (pH 6.8 or pH 8.2), 10 mM $Mg(CH_3CO_2)_2$, 1.5–1.8mM[γ-^{32}P]ATP (400–480Ci/mol), 0.09mMEGTA, 0.2mM $CaCl_2$, 7 mM β-mercaptoethanol, and either 7.7 nM $(\alpha\beta\gamma\delta)_4$ PhK or 30.8 nM $\alpha\gamma\delta$. The reactions were initiated by the addition of kinase and were carried out for 30 min at 30 °C. At 5 min intervals, two separate aliquots (20 μL each) from the reaction were quenched in parallel, either by spotting on P81 filter papers [followed by immersion in dilute phosphoric acid (0.5%)] or by dilution and rapid mixing in SDS buffer [62.5 mM Tris (pH 6.8), 10% glycerol, 2% SDS, 5% 2-mercaptoethanol, 0.05% Bromphenol blue]. Total incorporation of the ^{32}P label into the complex was determined by measuring radioactivity on the filter papers. The extent of incorporation of ^{32}P into the regulatory β and/or α subunits in each complex was assessed by resolving the subunits on 7.5% polyacrylamide gels and determining their relative intensities by autoradiography with a Typhoon 9410 Phosphor Imager (Amersham Biosciences, Piscataway, NJ). Autophosphorylation progress curves were derived from exponential fitting of the aforementioned time course data using the Origin 7.5 software package (OriginLab, Northampton, MA).

Activation by Autophosphorylation

The nonactivated $(\alpha\beta\gamma\delta)_4$ complexes (7.7 nM) and $\alpha\gamma\delta$ subcomplex (30.8 nM) were incubated in pH 8.2 autophosphorylation buffer (58 mM β-glycerophosphate/46 mM Tris, 0.08 mM EGTA, 5 mM β-mercaptoethanol) either alone (control) or in the presence of 0.18 mM $CaCl_2$, 9.1 mM $Mg(CH_3CO_2)_2$, and 2 mM ATP at 30 °C. After 20 min, aliquots from each reaction were removed and diluted 10-fold into pH 6.8 GP*b* conversion buffer (60 mM β-glycerophosphate/50 mM Tris, 0.22 mM $CaCl_2$, 0.1 mM EGTA, 10.9 mM $Mg(CH_3CO_2)_2$, 1.2 mM[γ-^{32}P]ATP (600 Ci/mol), 5mMβ-mercaptoethanol, and 25 μM GP*b*). At intervals of 2, 4, 8, and 12 min, 20 μL aliquots were removed from the reaction mixture to measure ^{32}P incorporation into GP*b* as described above.

Chemical Cross-linking and Partial Proteolysis of αγδ

Prior to cross-linking, His_6-$\alpha\gamma\delta$ was purified by size exclusion chromatography (Toyopearl HW-55F: 1.4 cm × 49 cm) in 50 mM Hepes buffer (pH 6.8), 0.1 mM EDTA, 200 mM NaCl, and 14 mM β-mercaptoethanol to remove glycerol and any high molecular weight aggregates formed during storage of the complex. Fractions containing $\alpha\gamma\delta$ were pooled,

dialyzed against cross-linking buffer [50 mM Hepes (pH 6.8), 0.1 mM EDTA] overnight, and concentrated by ultrafitration using a Centricon filter device (10 kDa MWCO; Millipore). Cross-linking of the αγδ subcomplex with formaldehyde and partial digestion of the α subunit with chymotrypsin in both the native and cross-linked complex were carried out as described for the RM PhK complex (28). Mapping of the region of α cross-linked to the catalytic γ subunit in the αγδ complex by formaldehyde was performed using previously established methods (29).

RESULTS

Subunit Stoichiometry of rPhK and the αγδ Subcomplex

Using a MultiBac expression system designed for heterologous, multisubunit protein complexes (30, 31), we have simultaneously expressed the α, β, γ, and δ subunits of the rabbit muscle PhK complex in Hi-5 cells using a single transfer vector, pFBDM-Hisα/β/γ/δ_{rabbit} (Figure 1).A separate rBV carrying the transfer vector pFBDM-Hisα/γ/δ_{rabbit} was also engineered and used to express the rabbit muscle αγδ subcomplex. The α subunit was constructed with an N-terminally attached hexa-His tag in both complexes to facilitate their purification (~90%and>95% for rPhK and αγδ, respectively) from extracts of BV-infected Hi-5 cells (Figure 2). Modification of the C-terminus of α was avoided because (1) it is part of a phosphorylatable regulatory region of the subunit that binds the catalytic γ subunit (29), (2) it has been covalently linked to the δ subunit in the intact complex (32), and (3) it contains an epitope for a subunit-specific anti-α mAb (13) beneficial in characterizing subunit interactions of α in the PhK complex (33). This C-terminal region of α is selectively cleaved by chymotrypsin in the PhK complex and is subject to the action of proteases in preparations of the enzyme from rabbit muscle (13, 28). Correspondingly, we observed that the minor impurities detected in purified rPhK (Figure 2, lane 2) were C-terminal cleavage products of α, based on their cross-reactivity against both anti-PhK guinea pig polyclonal antibodies (pAbs) and anti-penta-His mAbs (data not shown). The stoichiometry of α and the remaining subunits of rPhK (determined by scanning densitometry of gels containing the Coomassie-stained protein) was essentially identical to the RM PhK complex. The same method indicated a 1:1:1 stoichiometry for the α, γ, and δ subunits in the purified αγδ subcomplex. Corroborating these results, the apparent masses measured for rPhK (1.3×10^6 Da) and αγδ (2×10^5 Da) by size exclusion HPLC corresponded to theoretical masses calculated respectively for complexes having $(\alpha\beta\gamma\delta)_4$ and αγδ subunit stoichiometries. To evaluate the structural integrity of these complexes and their utility as models of RM PhK, we next measured their activities under conditions known to activate the native enzyme. All comparisons, except where noted, were made on the basis of mole amounts of the catalytic γ subunit in each complex, and all assays were carried out with at least three separate preparations of RM PhK, rPhK, and αγδ.

pH Dependence

The activation state of PhK is assessed by the ratio of its phosphotransferase activity at pH 6.8 versus pH 8.2, because activators bring about a large increase in activity at the former pH and little, or none, at the latter; however, the activity at both pH values remains fully Ca^{2+}-dependent (34). The catalytic activity of RM PhK at pH 8.2 is well-behaved and linear; in contrast, its activity at pH 6.8 is hysteretic, being characterized by autoactivation over a long lag period (16). At short assay times, the pH 6.8/8.2 ratio of activity reportedly ranges anywhere between 0.04 and 0.08 for purified RM PhK (9). The pH6.8/8.2 activity ratios observed herein for RM PhK(0.04) and rPhK (0.09) were similar (Figure 3), with the latter falling essentially in the upper range reported for the native RM complex. The small difference observed in the pH ratios for rPhK and RM PhK results primarily from the increased specific activity observed for rPhK at pH 6.8, rather than the minor difference

(25%) observed in their maximal activities at pH 8.2. Compared to pH 8.2, the phosphotransferase activity at pH 6.8 varies more among preparations of PhK from rabbit muscle, because it may be amplified by trace quantities of PhK activated by mechanisms other than increased pH, such as partial proteolysis and/or phosphorylation of the regulatory α and/or β subunits. Thus, the somewhat greater pH 6.8 activity of rPhK (Figure 3) could well be due to the slight proteolysis observed for the α subunits of rPhK(Figure 2). Minor differences in activation by phosphorylation of either the rPhK or RM PhK complex are also possible, because there are over 50 phosphorylation sites on α and β in the intact PhK complex that may be targeted to different extents by kinases in insect cells and mammalian muscle cells (8).

The MultiBac-expressed αγδ complex exhibited a pH-dependent activity ratio (pH6.8/8.2=0.15) that more closely reflected values observed for the hexadecameric complexes (0.04 and 0.09 for RM PhK and rPhK, respectively) than the value (0.46) determined for the αγδ trimer obtained following partial disruption of RM PhK by LiBr (35). At the activating pH 8.2, the specific activity of γ in the trimer was only 30% of the value measured for γ in the $(\alpha\beta\gamma\delta)_4$ RM PhK complex (Figure 3). Product formation catalyzed by αγδ at pH 8.2 was, however, linear over 30 min (data not shown), indicating that factors other than stability lead to lower catalytic efficiency of γ in the αγδ subcomplex at this pH. The specific activity measured for αγδ at pH 6.8 was similar to that of rPhK; however, in contrast to both $(\alpha\beta\gamma\delta)_4$ complexes, there was no lag time evident in its formation of product (Figure 4).

Hysteresis

Hysteretic enzymes are defined as those that exhibit a slow response to rapid changes in ligand concentration or a time lag in product formation (36). As discussed above, such a time lag has been observed for the conversion of GP*b* to GP*a* by nonactivated RM PhK at pH 6.8 in both Hepes (37) and Tris/β-glycerophosphate (β-GP) buffer systems (38). This property of RM PhK has been shown to be affected by a number of variables (37); thus, even though it is a common property of the nonactivated enzyme, the hysteretic time courses can vary even for a single enzyme preparation. As opposed to the $(\alpha\beta\gamma\delta)_4$ complex, however, neither the recombinant αγδ complex (Figure 4) nor the αγδ and γδ subcomplexes obtained by dissociation of PhK with LiBr exhibit lags in their GP*b* conversion reaction (39). Thus, the lag is a marker for subunit interactions that apparently occur only in the intact PhK complex and may perhaps require the participation of β subunits. A comparison of the reactions catalyzed by rPhK and RM PhK in Tris/β-GP at pH 6.8 demonstrated that both enzymes exhibit a lag in product formation, with both becoming increasingly more active with time (Figure 4).

Ca^{2+} Dependence

The absolute dependence of RM PhK on Ca^{2+} ions for its activity (34, 40) is attributed to the presence of the tightly bound intrinsic CaM subunit (δ) (1). With δ being present in both rPhK and αγδ, their activities were, as expected, Ca^{2+}-dependent; both complexes required the same concentration of Ca^{2+} as RM PhK to achieve full activation, namely, 5.5 μM, in assays carried out at pH 8.2 (Figure 5A). The activating concentration of Ca^{2+} observed for the recombinant complexes was also in close agreement with that reported for full activation of RM PhK at pH 8.2 in previous studies using alternative methods (34, 41–43). The shapes of the Ca^{2+}-titration curves for the recombinant enzymes were also very similar to that for RM PhK (Figure 5A). As shown by their Hill plots (Figure 5B),RM PhK and rPhK required similar concentrations of Ca^{2+} to achieve half-maximal activation ($[Ca^{2+}]_{0.5}$ =0.4 and 0.7 μM, respectively), whereas the αγδ complex required approximately three times the amount of Ca^{2+} to achieve half-maximal activity ($[Ca^{2+}]_{0.5}$ = 1.5 μM). As shown in Figure

5C, Ca^{2+} significantly increased the activities of the RM PhK (43-fold), rPhK (29-fold), and $\alpha\gamma\delta$ (16-fold) complexes, and at fully activating concentrations of Ca^{2+}, the specific activities of RM PhK and rPhK were similar, with the latter 75% of the former, whereas the peak activity measured for $\alpha\gamma\delta$ was only 30%of that measured for RM PhK when normalized per mole of γ. In contrast to the Ca^{2+}-loaded complexes, the specific activities measured for RM PhK, rPhK, and $\alpha\gamma\delta$ in the absence of free Ca^{2+} were low and nearly identical (Figure 5C), indicating that the Ca^{2+}-independent basal activity of the catalytic subunit is considerably less affected by the regulatory subunits than the Ca^{2+}-dependent activity, which is greatest when all three regulatory subunits are present. Consistent with this observation, allosterically activated PhK, whose activators act through the regulatory subunits, requires Ca^{2+} ions for activation to be observed.

The 16-fold stimulation of $\alpha\gamma\delta$ by Ca^{2+} is consistent with previous results from our laboratory demonstrating the presence of a Ca^{2+}-dependent subunit communication network involving the α, γ, and δ subunits in RM PhK (29). In that report it was shown that the C-terminal regulatory region of α binds to the C-terminal regulatory domain of γ (γCRD) and that cross-linking between these two domains in the PhK complex by the near-zero length cross-linker formaldehyde increases in the presence of Ca^{2+}, which presumably acts through binding to δ. To determine whether the connectivity observed between α and γ in the $(\alpha\beta\gamma\delta)_4$ complex is preserved in the $\alpha\gamma\delta$ complex, the trimer was similarly cross-linked with formaldehyde in the absence and presence of Ca^{2+}, resulting in the formation of an αγ dimer, with the extent of its formation also increased (20%) by Ca^{2+} (magnified insert, Figure 6A). To map the regions of α cross-linked to γ in αγδ, control and cross-linked trimers were partially digested with chymotrypsin, which selectively cleaves α in the $(\alpha\beta\gamma\delta)_4$ RM PhK complex and releases 24 and 58 kDa C-terminal fragments of that subunit, termed respectively α_{f1} and α_{f2} (28). Both fragments contain a known epitope for an anti-α subunit-specific mAb that has been used previously to identify the location of the epitope in the PhK complex (13) and the presence of the α subunit in cross-linked conjugates from PhK (28, 29). A comparison of the digests of the control and cross-linked $\alpha\gamma\delta$ trimers revealed two new bands (Figure 6, lanes 5), termed α_{f1}-γ ($mass_{theor}$ = 69.7 kDa; 3.9% error) and α_{f2}-γ ($mass_{theor}$ = 102.7 kDa; 2.6% error), which correspond by both apparent mass and cross-reactivity against subunit-specific mAbs to cross-linking between the catalytic γ subunit ($mass_{theor}$ = 44.7 kDa) and the C-terminal chymotryptic fragments of α(α_{f1} andα_{f2}). Thus, the near-zero length, Ca^{2+}-dependent cross-linking of γ to the C-terminal regulatory domain of α within the trimer is consistent with the Ca^{2+}-dependent cross-linking between these two subunits in RM PhK (29). The sum of the data in this section demonstrates that the Ca^{2+}-dependent subunit interactions observed for the $\alpha\gamma\delta$ complex are nearly identical to those detected for the α, γ, and δ subunits in RM PhK and that the $\alpha\gamma\delta$ trimer is an excellent model for studying the structure and function of these subunits in the hexadecameric PhK complex, especially as related to the effects of Ca^{2+} ions.

Autophosphorylation and Autoactivation

Autophosphorylation of its α and β subunits is an intrinsic activity of RM PhK (44), the rate of which is affected by several factors, including buffers, cations, and pH, with greater activity at slightly alkaline pH (16, 45, 46). The recombinant complexes were examined for this pH-sensitive activity by measuring the time-dependent incorporation of radioactivity from [γ-^{32}P]ATP into the α and β subunits at pH 6.8 and 8.2. The extent of incorporation of ^{32}P into the regulatory subunits was compared on the basis of equivalent molar amounts of the α subunit added for each complex per gel lane (Figure 7). Going from pH 6.8 to pH 8.2, both RM PhK and rPhK exhibited large and roughly equivalent increases in autophosphorylation of their α subunits and smaller increases in autophosphorylation of

their β subunits (Figure 7A,B). As was the case with GP*b* conversion (Figure 3), autophosphorylation of the α subunit in the $\alpha\gamma\delta$ subcomplex was less stimulated by increasing pH (Figure 7C) than in the $(\alpha\beta\gamma\delta)_4$ complex.

The autophosphorylation of RM PhK leads to an increase in its activity measured at pH 6.8 (44). To determine the effects of autophosphorylation on the activation of γ in the recombinant complexes, autophosphorylation of each complex was carried out for 20min at pH8.2, and the GP*b* conversion activities of the phosphorylated and nonphosphorylated control complexes at pH 6.8 were then measured at the indicated times (Figure 8). The concentrations of ATP and all other assay components were adjusted in the control reactions to match carryover of components from the autophosphorylation reactions. At the earliest time point (2 min), the activation of the rPhK and the RM PhK was roughly equivalent at 3- and 4-fold, respectively, with the amount of activation for each decreasing at longer assay times due to hysteresis in the nonphosphorylated control reactions. Autophosphorylation of the α subunit within the $\alpha\gamma\delta$ subcomplex also brought about activation of the trimer by ~2-fold (Figure 8C). These findings suggest a structural linkage between α and γ and are consistent with their cross-linking by the near zero-length cross-linker formaldehyde (ref 29 and results herein) and by other cross-linkers acting on the $(\alpha\beta\gamma\delta)_4$ complex (28, 29, 33, 47, 48).

DISCUSSION

The properties of the expressed rPhK described herein closely mimic those of RM PhK, including activity at pH 8.2, ratio of activities at pH 6.8 versus pH 8.2, hysteretic activity at pH 6.8, Ca^{2+} dependence, and activation by phosphorylation. Because this expressed hexadecamer retains the key regulatory properties of the purified RM PhK, it is well-suited as a model to now allow the first structure–function studies on the regulation of the holoenzyme using site-directed mutagenesis. Given that only 10% at most of PhK's mass is devoted to its catalytic activity, i.e., the catalytic core of its γ subunit, it is of high import to understand the structural underpinnings of its regulation by diverse activators. The catalytic core itself also has some intriguing potential regulatory features of its own, including four inserts not found in the closely related PKA. The first of these is an insert of 20 residues at its N-terminus, followed by an acidic hexamer at 60–65, a hydrophilic hexamer at 196–201, and an acidic tetramer at 252–255 (7, 49). All four of these inserts are located at the periphery of the catalytic core structure (49) and may be regions through which the catalytic domain may communicate with PhK's regulatory subunits. Another important regulatory feature of the catalytic subunit is a large region of ~97 residues at its C-terminus, which is discussed below. Of its regulatory subunits, little is known regarding key regulatory features of the large, homologous α and β subunits, other than their important phosphorylation sites near the C-terminal region of α and at the N-terminal of β. It will be of special interest to evaluate the missense mutations in these two large subunits that give rise to glycogen storage disease. Although most of the known mutations occur in the liver isoform of PhK (50–53), many are conserved in the muscle isoform. The effects of disease-causing missense mutations on the assembly, activity, and regulation of PhK can now be evaluated using this BV-mediated expression system.

The general region of the γ subunit thought to interact with CaM (δ subunit) was initially localized to its C-terminal one-quarter (residues 290–386) by truncation (54), cross-linking (32), and synthetic peptides (55). We refer to this region of γ as its C-terminal regulatory domain, or γCRD. The truncated γ subunit missing the γCRD is fully active but insensitive to Ca^{2+}/CaM(54). Screening of the γCRD for potential high-affinity CaM-binding sequences through the use of overlapping synthetic peptides revealed two distinct, nonoverlapping CaM-binding domains (55). The more N-terminal of these contains regions

of high sequence similarity to skeletal muscle troponin I (55–57), including its functional "inhibitory peptide" (58) that interacts with troponin C or actin in a Ca^{2+}-dependent manner (59, 60). Through zero-length cross-linking, we have shown an Asp-Lys salt bridge within the PhK complex between δ and the TnI-like domain of γ (32). Within the PhK complex there is also an α ↔ γ ↔ δ communication network through which the binding of Ca^{2+}, presumably to the δ subunit, causes distant conformational changes at the C-terminal regulatory region of the α subunit (29, 61). The region of γ that has been shown to interact with this regulatory region of α is the γCRD, distal to its CaM-binding regions, and it has been hypothesized that the Ca^{2+}-dependent allosteric switch involving actin–troponin I–troponin C that is mediated by the troponin I inhibitory peptide may be mimicked by the α–γCRD–δ intersubunit network of PhK, with α functionally representing actin (29, 32). That the expressed αγδ subcomplex described herein retains the appropriate Ca^{2+}-dependent activity will allow the above hypothesis to be evaluated in a simple system containing only the three pertinent subunits. The γCRD has also been shown to cross-link to the N-terminal regulatory region of β, and the possibility was raised that this region of γ is the master allosteric activation switch governing the entire PhK complex (62). This notion can now be assessed using rPhK having the key regulatory properties of RM PhK.

It was thought that the differences in the properties of the previously expressed PhK and RM PhK might be due to differences in the posttranslational modifications catalyzed by rabbit muscle versus insect cells (8). Besides their potentially different phosphorylation, the α and β subunits are farnesylated in muscle (63), and it has been observed for other proteins that improper prenylationmay occur in insect expression systems (64). That the properties of RM PhK and rPhK so closely match each other in this study suggests that the previously observed differences were more likely due to the use of the β subunit from rabbit and the α and γ subunits from rat (8), noting that the last two subunits share only 94% and 92% identity with their rabbit counterparts.

Supplementary Material

Refer to Web version on PubMed Central for supplementary material.

Acknowledgments

I.G.B. dedicates this work to Professor G. A. Kochetov, advisor and mentor, A. N. Belozersky Institute of Physicochemical Biology, Moscow State University, Russia. We are thankful to Dr. A. Ladokhin for providing the Spex Fluorolog 322, to Dr. A. Fenton for use of the PTI spectrofluorometer, to Dr. W. Liu for help with HPLC, and to Dr. E. Posokhov, Dr. M. Rodnin, and Dr. O. Kyrychenko (all from KUMC) for help with fluorescence measurements and valuable advice.

References

1. Cohen P, Burchell A, Foulkes JG, Cohen PTW. Identification of the Ca^{2+}-dependent modulator protein as the fourth subunit of rabbit skeletal muscle phosphorylase kinase. FEBS Lett. 1978; 92:287–293. [PubMed: 212300]
2. Brushia RJ, Walsh DA. Phosphorylase kinase: the complexity of its regulation is reflected in the complexity of its structure. Front Biosci. 1999; 4:D618–D641. [PubMed: 10487978]
3. Ramachandran C, Goris J, Waelkens E, Merlevede W, Walsh DA. The interrelationship between cAMP-dependent α and β subunit phosphorylation in the regulation of phosphorylase kinase activity. Studies using subunit specific phosphatases. J Biol Chem. 1987; 262:3210–3218. [PubMed: 3029103]
4. Zander NF, Meyer HE, Hoffmann-Posorske E, Crabb JW, Heilmeyer LMG Jr, Kilimann MW. cDNA cloning and complete primary structure of skeletal muscle phosphorylase kinase (alpha subunit). Proc Natl Acad Sci USA. 1988; 85:2929–2933. [PubMed: 3362857]

5. Kilimann MW, Zander NF, Kuhn CC, Crabb JW, Meyer HE, Heilmeyer LMG Jr. The alpha and beta subunits of phosphorylase kinase are homologous: cDNA cloning and primary structure of the beta subunit. Proc Natl Acad Sci USA. 1988; 85:9381–9385. [PubMed: 3200826]
6. Grand RJA, Shenolikar S, Cohen P. The amino acid sequence of the δ subunit (calmodulin) of rabbit skeletal muscle phosphorylase kinase. Eur J Biochem. 1981; 113:359–367. [PubMed: 7202416]
7. Reimann EM, Titani K, Ericsson LH, Wade RD, Fischer EH, Walsh DA. Homology of the gamma subunit of phosphorylase *b* kinase with cAMP-dependent protein kinase. Biochemistry. 1984; 23:4185–4192. [PubMed: 6541504]
8. Kumar P, Brushia RJ, Hoye E, Walsh DA. Baculovirus-mediated overexpression of the phosphorylase *b* kinase holoenzyme and $\alpha\gamma\delta$ and $\gamma\delta$ subcomplexes. Biochemistry. 2004; 43:10247–10254. [PubMed: 15287752]
9. Pickett-Gies, CA.; Walsh, DA. Phosphorylase Kinase, in The Enzymes. 3. Boyer, PD.; Krebs, EG., editors. Vol. XVII. Academic Press; San Diego, CA: 1986. p. 395-459.
10. Nairn AC, Grand RJ, Perry SV. The amino acid sequence of rabbit skeletal muscle calmodulin. FEBS Lett. 1984; 167:215–220. [PubMed: 6698209]
11. Chien YH, Dawid IB. Isolation and characterization of calmodulin genes from *Xenopus laevis*. Mol Cell Biol. 1984; 4:507–513. [PubMed: 6325880]
12. Jentoft N, Dearborn DG. Labeling of proteins by reductive methylation using sodium cyanoborohydride. J Biol Chem. 1979; 254:4359–4365. [PubMed: 571437]
13. Wilkinson DA, Marion TN, Tillman DM, Norcum MT, Hainfeld JF, Seyer JM, Carlson GM. An epitope proximal to the carboxyl terminus of the α-subunit is located near the lobe tips of the phosphorylase kinase hexadecamer. J Mol Biol. 1994; 235:974–982. [PubMed: 7507177]
14. Wilkinson DA, Norcum MT, Fizgerald TJ, Marion TN, Tillman DM, Carlson GM. Proximal regions of the catalytic gamma and regulatory beta subunits on the interior lobe face of phosphorylase kinase are structurally coupled to each other and with enzyme activation. J Mol Biol. 1997; 265:319–329. [PubMed: 9018046]
15. Fisher EH, Krebs EG. The isolation and crystallization of rabbit skeletal muscle phosphorylase *b*. J Biol Chem. 1958; 231:65–71. [PubMed: 13538948]
16. King MM, Carlson GM. Synergistic activation by Ca^{2+} and Mg^{2+} as the primary cause for hysteresis in the phosphorylase kinase reactions. J Biol Chem. 1981; 256:11058–11064. [PubMed: 6793591]
17. Kastenschmidt LL, Kastenschmidt J, Helmreich EJM. Subunit interactions and their relationship to the allosteric properties of rabbit skeletal muscle phosphorylase *b*. Biochemistry. 1968; 7:3590–3608. [PubMed: 5681467]
18. Cohen P. The subunit structure of rabbit skeletal muscle phosphorylase kinase, and the molecular basis of its activation reactions. Eur J Biochem. 1973; 34:1–14. [PubMed: 4349654]
19. Choi JK, Yoon SH, Hong HY, Choi DK, Yoo GS. A modified Coomassie blue staining of proteins in polyacrylamide gels with Bismark brown R. Anal Biochem. 1996; 236:82–84. [PubMed: 8619499]
20. Roskoski R Jr. Assays of protein kinase. Methods Enzymol. 1983; 99:3–6. [PubMed: 6316096]
21. Paudel HK, Xu YH, Jarrett HW, Carlson GM. The model calmodulin-binding peptide melittin inhibits phosphorylase kinase by interacting with its catalytic center. Biochemistry. 1993; 32:11865–11872. [PubMed: 8218258]
22. Boulatnikov IG, Nadeau OW, Daniels PJ, Sage JM, Jeyasingham MD, Villar MT, Artigues A, Carlson GM. The regulatory β subunit of phosphorylase kinase interacts with glyceraldehyde-3-phosphate dehydrogenase. Biochemistry. 2008; 47:7228–7236. [PubMed: 18549242]
23. Tsien RY. New calcium indicators and buffers with high selectivity against magnesium and protons: design, synthesis, and properties of prototype structures. Biochemistry. 1980; 19:2396–2404. [PubMed: 6770893]
24. Minta A, Kao JPY, Tsien RY. Fluorescent indicators for cytosolic calcium based on rhodamine and fluorescein chromophores. J Biol Chem. 1989; 264:8171–8178. [PubMed: 2498308]
25. Grynkiewicz G, Poenie M, Tsien RY. A new generation of Ca^{2+} indicators with greatly improved fluorescence properties. J Biol Chem. 1985; 260:3440–3450. [PubMed: 3838314]

26. Tsien, RY. Monitoring Cell Calcium, in Calcium as a Cellular Regulator. Carafoli, E.; Klee, C., editors. Oxford University Press; Cary, NC: 1998. p. 28-54.
27. White C, McGeown JG. Regulation of basal intracellular calcium concentration by the sarcoplasmic reticulum in myocytes from the rat gastric antrum. J Physiol. 2000; 529:395–404. [PubMed: 11101649]
28. Nadeau OW, Traxler KW, Fee LR, Baldwin BA, Carlson GM. Activators of phosphorylase kinase alter the cross-linking of its catalytic subunit to the C-terminal one-sixth of its regulatory α subunit. Biochemistry. 1999; 38:2551–2559. [PubMed: 10029550]
29. Rice NA, Nadeau OW, Yang Q, Carlson GM. The calmodulin-binding domain of the catalytic γ subunit of phosphorylase kinase interacts with its inhibitory α subunit. J Biol Chem. 2002; 277:14681–14687. [PubMed: 11847235]
30. Berger I, Fitzgerald DJ, Richmond TJ. Baculovirus expression system for heterologous multiprotein complexes. Nat Biotechnol. 2004; 22:1583–1587. [PubMed: 15568020]
31. Fitzgerald DJ, Berger P, Schaffitzel C, Yamada K, Richmond TJ, Berger I. Protein complex expression by using multigene baculoviral vectors. Nat Methods. 2006; 3:1021–1032. [PubMed: 17117155]
32. Jeyasingham MD, Artigues A, Nadeau OW, Carlson GM. Structural evidence for co-evolution of the regulation of contraction and energy production in skeletal muscle. J Mol Biol. 2008; 377:623–629. [PubMed: 18281058]
33. Nadeau OW, Sacks DB, Carlson GM. The structural effects of endogenous and exogenous Ca^{2+}/calmodulin on phosphorylase kinase. J Biol Chem. 1997; 272:26202–26209. [PubMed: 9334188]
34. Brostrom CO, Hunkeler FL, Krebs EG. The regulation of skeletal muscle phosphorylase kinase by Ca^{2+} J Biol Chem. 1971; 246:1961–1967. [PubMed: 5549597]
35. Chan JKF, Graves DJ. Isolation and physicochemical properties of active complexes of rabbit muscle phosphorylase kinase. J Biol Chem. 1982; 257:5939–5947. [PubMed: 6802824]
36. Frieden C. Kinetic aspects of regulation of metabolic processes. The hysteretic enzyme concept. J Biol Chem. 1970; 245:5788–5799. [PubMed: 5472372]
37. Kim G, Graves DJ. On the hysteretic response of rabbit skeletal muscle phosphorylase kinase. Biochemistry. 1973; 12:2090– 2095. [PubMed: 4735880]
38. Krebs EG, Love DS, Bratvold GE, Trayser KA, Meyer WL, Fischer EH. Purification and properties of rabbit skeletal muscle phosphorylase *b* kinase. Biochemistry. 1964; 3:1022–1033. [PubMed: 14220660]
39. Chan JKF, Graves DJ. Rabbit skeletal muscle phosphorylase kinase. Catalytic and regulatory properties of the active αγδ and γδ complexes. J Biol Chem. 1982; 257:5948–5955. [PubMed: 6279620]
40. Meyer WL, Fisher EH, Krebs EG. Activation of skeletal muscle phosphorylase *b* kinase by Ca. Biochemistry. 1964; 3:1033–1039. [PubMed: 14220661]
41. Cohen P. Phosphorylation of rabbit skeletal muscle phosphorylase kinase by cyclic GMP-dependent protein kinase. FEBS Lett. 1980; 119:301–306. [PubMed: 6253325]
42. Burger D, Cox JA, Fischer EH, Stein EA. The activation of rabbit skeletal muscle phosphorylase kinase requires the binding of 3 Ca^{2+} per delta subunit. Biochem Biophys Res Commun. 1982; 105:632–638. [PubMed: 7092874]
43. Kilimann MW, Heilmeyer LMG Jr. Multiple activities on phosphorylase kinase. 1 Characterization of three partial activities by their response to calcium ion, magnesium ion, pH, and ammonium chloride and effect of activation by phosphorylation and proteolysis. Biochemistry. 1982; 21:1727–1734. [PubMed: 6282317]
44. DeLange RJ, Kemp RG, Riley WD, Cooper RA, Krebs EG. Activation of skeletal muscle phosphorylase kinase by adenosine triphosphate and adenosine 3′,5′-monophosphate. J Biol Chem. 1968; 243:2200–2208. [PubMed: 4296832]
45. Carlson GM, Graves DJ. Stimulation of phosphorylase kinase autophosphorylation by peptide analogs of phosphorylase. J Biol Chem. 1976; 251:7480–7486. [PubMed: 1002697]
46. Wang JH, Stull JT, Huang TS, Krebs EG. A study on the autoactivation of rabbit muscle phosphorylase kinase. J Biol Chem. 1976; 251:4521–4527. [PubMed: 947893]

47. Nadeau OW, Sacks DB, Carlson GM. Differential affinity cross-linking of phosphorylase kinase conformers by the geometric isomers of phenylenedimaleimide. J Biol Chem. 1997; 272:26196–26201. [PubMed: 9334187]
48. Ayers NA, Nadeau OW, Read MW, Ray P, Carlson GM. Effector-sensitive cross-linking of phosphorylase *b* kinase by the novel cross-linker 4-phenyl-1,2,4-triazoline-3,5-dione. Biochem J. 1998; 331:137–141. [PubMed: 9512471]
49. Owen DJ, Noble ME, Garman EF, Papageorgiou AC, Johnson LN. Two structures of the catalytic domain of phosphorylase kinase: an active protein kinase complexed with substrate analogue and product. Structure. 1995; 3:467–482. [PubMed: 7663944]
50. Burwinkel B, Shin YS, Bakker HD, Deutsch J, Lozano MJ, Maire I, Kilimann MW. Mutation hotspots in the PHKA2 gene in X-linked liver glycogenosis due to phosphorylase kinase deficiency with atypical activity in blood cells (XLG2). Hum Mol Genet. 1996; 5:653–658. [PubMed: 8733134]
51. Hendrickx J, Lee P, Keating JP, Carton D, Sardharwalla IB, Tuchman M, Baussan C, Willems PJ. Complete genomic structure and mutational spectrum of PHKA2 in patients with x-linked liver glycogenosis type I and II. Am J Hum Genet. 1999; 64:1541–1549. [PubMed: 10330341]
52. Burwinkel B, Hu B, Schroers A, Clemens PR, Moses SW, Shin YS, Pongratz D, Vorgerd M, Killimann MW. Muscle glycogenosis with low phosphorylase kinase activity: mutations in PHKA1, PHKG1 or six other candidate genes explain only a minority of cases. Eur J Hum Genet. 2003; 11:516–526. [PubMed: 12825073]
53. Beauchamp NJ, Dalton A, Ramaswami U, Niinikoski H, Mention K, Kenny P, Kolho KL, Raiman J, Walter J, Treacy E, Tanner S, Sharrard M. Glycogen storage disease type IX: high variability in clinical phenotype. Mol Genet Metab. 2007; 92:88–99. [PubMed: 17689125]
54. Harris W, Malencik DA, Johnson CM, Carr SA, Roberts GD, Byles CA, Anderson SR, Heilmeyer LMG Jr, Fisher EH, Crabb JW. Purification and characterization of catalytic fragments of phosphorylase kinase γ subunit missing a calmodulin-binding domain. J Biol Chem. 1990; 265:11740–11745. [PubMed: 2365696]
55. Dasgupta M, Honeycutt T, Blumenthal DK. The γ-subunit of skeletal muscle phosphorylase kinase contains two noncontiguous domains that act in concert to bind calmodulin. J Biol Chem. 1989; 264:17156–17163. [PubMed: 2507540]
56. Buschmeier B, Meyer HE, Mayr GW. Characterization of the calmodulin-binding sites of muscle phosphofructokinase and comparison with known calmodulin-binding domains. J Biol Chem. 1987; 262:9454–9462. [PubMed: 2954960]
57. Paudel HK, Carlson GM. Functional and structural similarities between the inhibitory region of troponin I coded by exon VII and the calmodulin-binding regulatory region of the catalytic subunit of phosphorylase kinase. Proc Natl Acad Sci USA. 1990; 87:7285–7289. [PubMed: 2402508]
58. Syska H, Wilkinson JM, Grand RJ, Perry SV. The relationship between biological activity and primary structure of troponin I from white skeletal muscle of the rabbit. Biochem J. 1976; 153:375–387. [PubMed: 179535]
59. Grand RJ, Levine BA, Perry SV. Proton-magnetic-resonance studies on the interaction of rabbit skeletal-muscle troponin I with troponin C and actin. Biochem J. 1982; 203:61–68. [PubMed: 7103951]
60. Vinogradova MV, Stone DB, Malanina GG, Karatzaferi C, Cooke R, Mendelson RA, Fletterick RJ. Ca^{2+}regulated structural changes in troponin. Proc Natl Acad Sci USA. 2005; 102:5038–5043. [PubMed: 15784741]
61. Nadeau OW, Carlson GM, Gogol EP. A Ca^{2+}-dependent global conformational change in the 3D structure of phosphorylase kinase obtained from electron microscopy. Structure. 2002; 10:23–32. [PubMed: 11796107]
62. Nadeau OW, Anderson DW, Yang Q, Artigues A, Paschall JE, Wyckoff GJ, McClintock JL, Carlson GM. Evidence for the location of the allosteric activation switch in the multisubunit phosphorylase kinase complex from mass spectrometric identification of chemically crosslinked peptides. J Mol Biol. 2007; 365:1429–1445. [PubMed: 17123541]
63. Heilmeyer LMG Jr, Serwe M, Weber C, Metzger J, Hoffman-Posorske E, Mayer HE. Farnesylcysteine, a constituent of the alpha and beta subunits of rabbit skeletal muscle

phosphorylase kinase: localization by conversion to S-ethylcysteine and by tandem mass spectrometry. Proc Natl Acad Sci USA. 1992; 89:9554–9558. [PubMed: 1409665]

64. Cha K, Bruel C, Inglese J, Khorana HG. Rhodopsin kinase: expression in baculovirus-infected insect cells, and characterization of post-translational modifications. Proc Natl Acad Sci US A. 1997; 94:10577–10582.

65. O'Reilly, DR.; Miller, LK.; Luckow, VA. Baculovirus expression vectors: a laboratory manual. Oxford University Press; New York: 1994. p. 124-158.

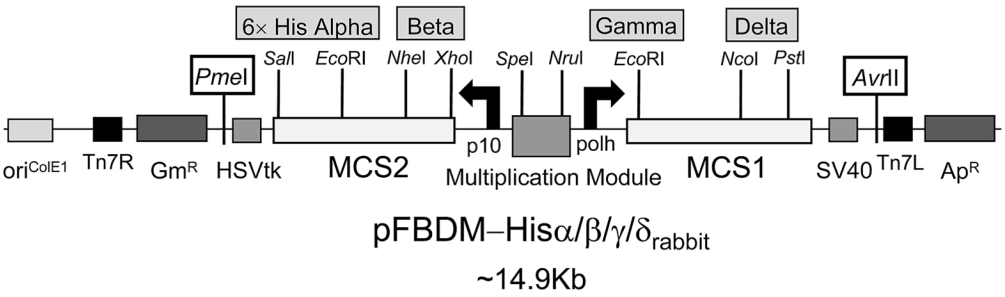

Figure 1.

Expression cassette for the recombinant PhK holoenzyme. The BV transfer vector pFBDM was used to express the cDNAs encoding the α, *β*, *γ*, and *δ* subunits of PhK. Following modification of theMCS1 and MCS2, the *δ* subunit was cloned into MCS1 using *Nco*I and *Pst*I restriction sites, and the α subunit was cloned intoMCS2 using *Sal*I and *Eco*RI restriction sites. The original pFBDM vector was modified to accommodate the catalytic *γ* and regulatory *β* subunit cDNAs, which were then cloned intoMCS1 and MCS2, respectively, using restriction sites *Eco*RI for *γ* and *Nhe*I and *Xho*I for *β*. Through the use of the *Spe*I and *Nru*I restriction sites in the multiplication module and unique restriction sites, *Pme*I and *Avr*II, the separate pFBDM vectors expressing different subunits were combined into a single large construct containing both ampicillin (Ap^R) and gentamycin (Gm^R) resistant markers. Expression of the α and *β* subunit pairs and the *γ* and *δ* subunit pairs is driven and terminated, respectively, by the p10 and polh very late viral promoters and the HSVtk and SV40 poly(A) signal sequences. The expression cassette for the recombinant α*γδ* was constructed in the same manner, except that the *β* subunit was not cloned into the MCS2.

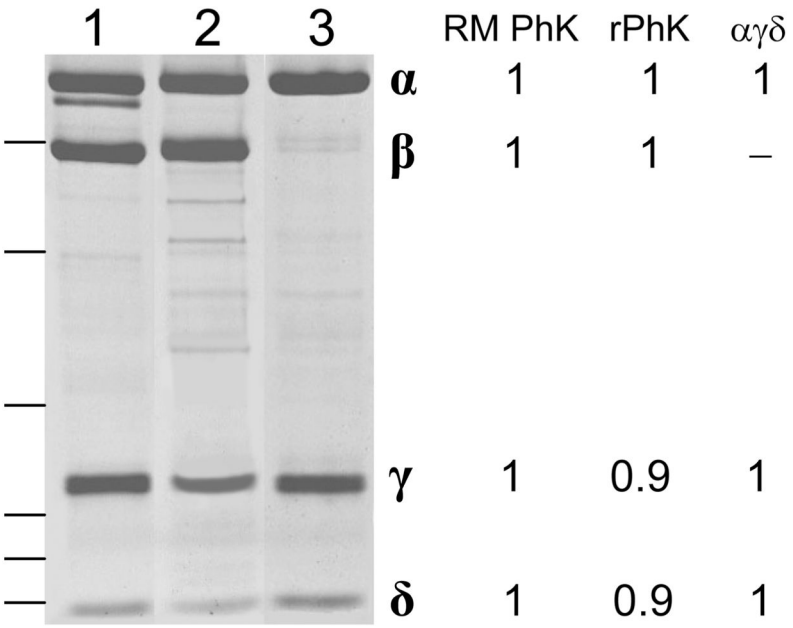

Figure 2.

SDS–PAGE and densitometric analyses of the RM PhK, rPhK, and $\alpha\gamma\delta$ complexes. RM PhK(lane 1), rPhK(lane 2), and $\alpha\gamma\delta$ (lane 3) were purified, resolved on 6–18% gradient polyacrylamide slab gels, and stained with Coomassie blue as described in Experimental Procedures. The molar ratios of the subunits (determined by their optical density) are indicated numerically to the right of the gel for each complex. The small band migrating directly under the α subunit of RM PhK (lane 1) is the α' isoform found in the small amount of red muscle in the white muscle tissue preparation (18). Molecular weight standards are indicated by lines to the left of the gel in order of decreasing molecular weight: β-galactosidase (116200), bovine serum albumin (84800), ovalbumin (53900), carbonic anhydrase (37400), soybean trypsin inhibitor (29100), and lysozyme (19800).

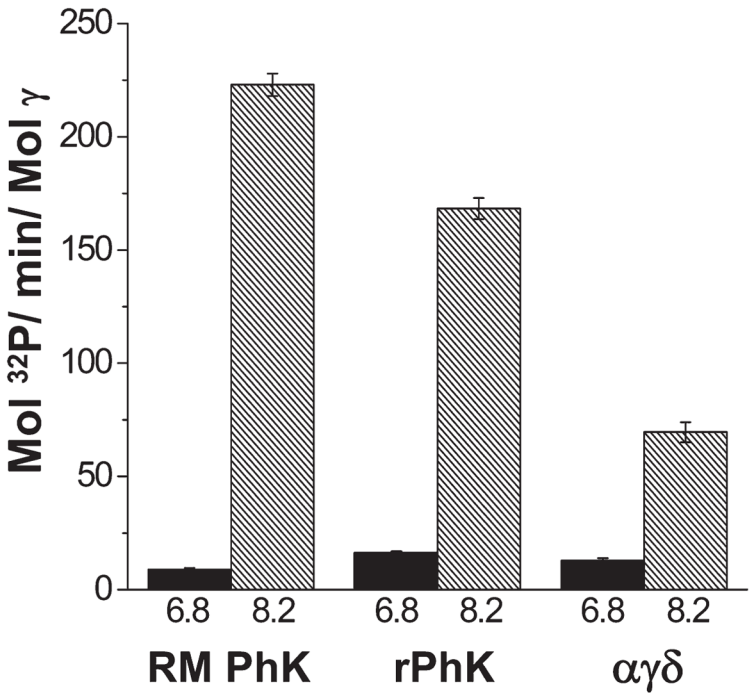

Figure 3.

Specific activity of the RM PhK, rPhK, and $\alpha\gamma\delta$ complexes at pH 6.8 and 8.2. The activities for RM PhK, rPhK, and $\alpha\gamma\delta$ were compared on the basis of the molar amount of catalytic subunit calculated for each complex using the method described under Figure 2. The specific activities indicated represent the mean ± SD for $n \geq 3$ trials.

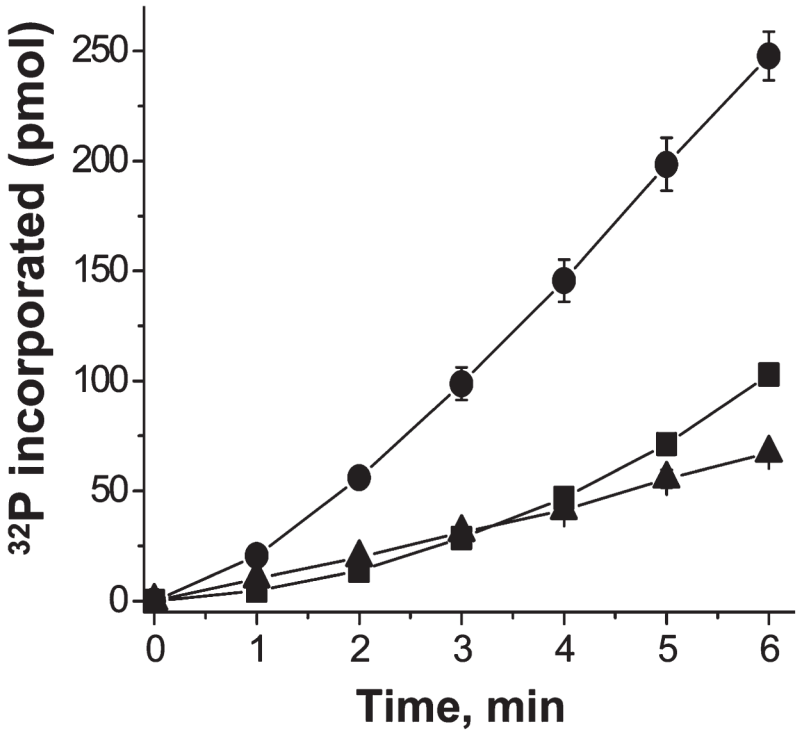

Figure 4.

Time course of GP*b* conversion by RM PhK, rPhK, and α*γδ*. Incorporation of [^{32}P]P_i into GP*b* by RM PhK (■), rPhK (●), and α*γδ* (▲) was measured at nonactivating pH(6.8) at the indicated times as described in Experimental Procedures. Measurements at each time point were carried out in triplicates and are represented as the mean ± SD.

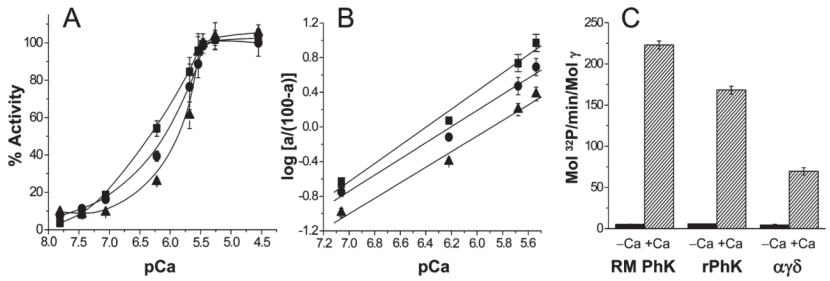

Figure 5.

Comparison of the Ca^{2+}-dependent activities of the RM PhK, rPhK, and $\alpha\gamma\delta$ complexes at pH8.2. (A) RM PhK(■), rPhK (●), and $\alpha\gamma\delta$ (▲) GP*b* conversion assays were carried out for 5 min with increasing concentrations of Ca^{2+} (see Experimental Procedures). (B) Corresponding Hill plot for data shown under panel A. (C) Specific activity measured for each complex at zero free Ca^{2+} (BAPTA only) and 28.2 μMCa^{2+}. Each bar represents the mean ± SD for $n \geq 3$ measurements.

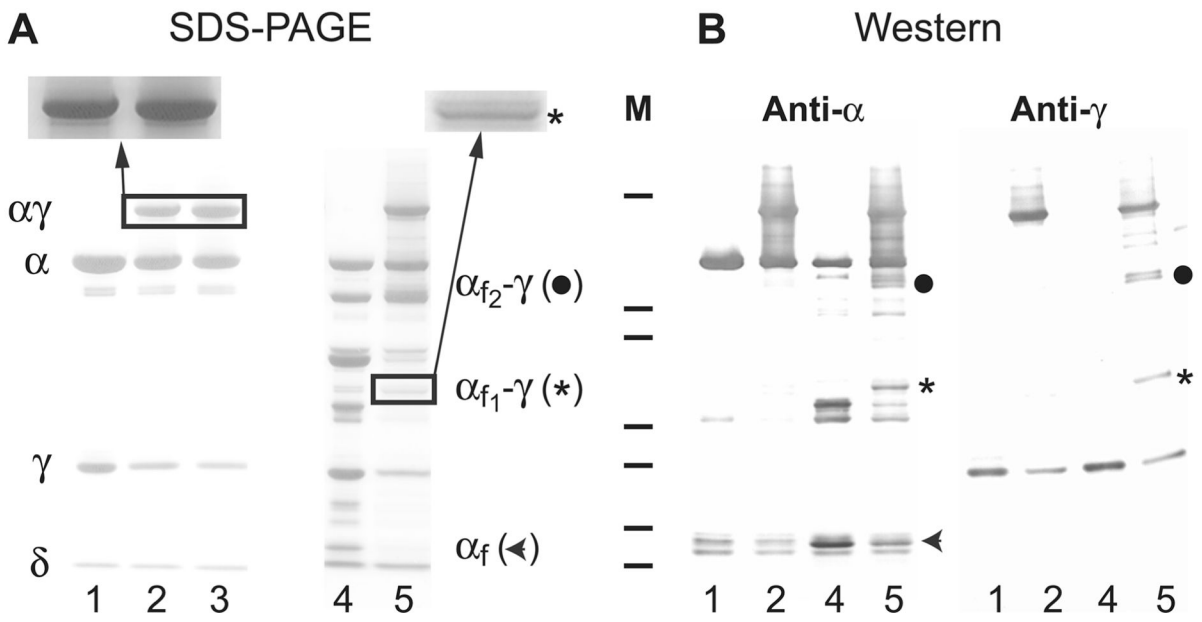

Figure 6.

Cross-linking and chymotryptic analyses of the recombinant $\alpha\gamma\delta$ trimer. (A) Native $\alpha\gamma\delta$ (lane 1) was cross-linked with formaldehyde in the absence (lane 2) and presence (lane 3) of the activating PhK ligand, Ca^{2+}, resolved by SDS–PAGE, and stained with Coomassie blue. A Ca^{2+}-dependent increase (20% by densitometry) in the extent formation of $\alpha\gamma$ is shown magnified (indicated by box and arrow) above lanes 1–3. Chymotryptic digestion of the ligand-free native (lane 4) and cross-linked (lane 5) forms of $\alpha\gamma\delta$ under identical conditions (see Experimental Procedures) revealed the formation of two new bands: the first magnified above lane 5 and labeled α_{f1}-γ (*) and the second designated α_{f2}-γ (●), with apparent masses of 66 and 100 kDa, respectively. (B) In parallel samples transferred to PVDF membranes and probed with subunit-specific mAbs against the α, γ, and δ subunits (data for the latter mAb not shown), both α_{f1}-γ and α_{f2}-γ cross-reacted only with anti-γ and anti-α mAbs, the latter of which binds an epitope located on the C-terminal one-sixth (24kDa) of α (α_f, arrowhead) (13). The new bands corresponded by both mass and cross-reactivity with subunit-specific mAbs to cross-linking between the γ subunit (44.7 kDa) and known C-terminal 24 kDa (α_{f1}) and 58 kDa (α_{f2}) chymotryptic fragments of α (13, 28). Lane M denotes molecular mass markers with masses in kDa corresponding to 206, 118, 97, 55, 38, 29, and 17, progressing from the top to the bottom of the gel.

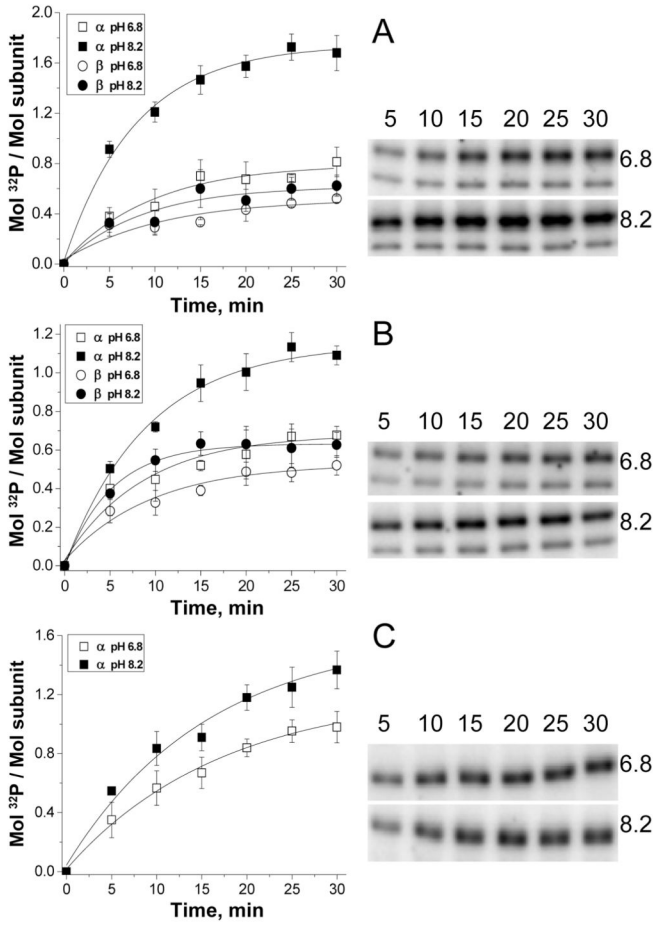

Figure 7.

Time- and pH-dependent autophosphorylation of RM PhK, rPhK, and $\alpha\gamma\delta$. Total phosphate incorporation into the RM PhK (A), rPhK (B), and $\alpha\gamma\delta$ (C) complexes at pH 6.8 and 8.2 was determined at the indicated times using [γ-^{32}P]ATP and a standard filter paper assay (21). In parallel experiments, the indicated phosphorylatable subunits of each complex were resolved by SDS–PAGE, and their relative intensities were subsequently determined by autoradiography. At the given time points, the fractional incorporation of phosphate into each subunit was determined as described under Experimental Procedures. The error bars reflect the mean of triplicate determinations (±SD) for the total incorporation of phosphate determined for each complex. Data fittings were carried out using the Origin 7.5 software package.

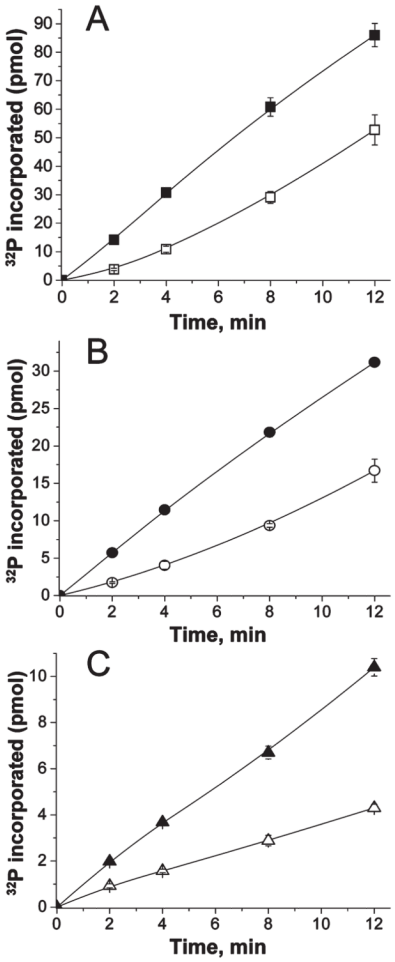

Figure 8.

Activation of the RM PhK, rPhK, and $\alpha\gamma\delta$ complexes by autophosphorylation. RM PhK (A), rPhK (B), and $\alpha\gamma\delta$ (C) were incubated with either +Ca^{2+}/Mg^{2+}/ATP or buffer at pH 8.2 for 20 min. Aliquots of the solutions containing RM PhK[buffer (□); Ca^{2+}/Mg^{2+}/ATP (■)], rPhK [buffer (○); Ca^{2+}/Mg^{2+}/ATP (●)], and $\alpha\gamma\delta$ [buffer (△); Ca^{2+}/Mg^{2+}/ATP (▲)] were then diluted 10-fold into an assay mixture buffered at nonactivating pH 6.8. At the indicated times, aliquots were removed for determination of ^{32}P incorporation into GP*b* as described under Experimental Procedures. The error bars reflect the mean of triplicate assays (±SD) for the total incorporation of phosphate into GP*b* at each time point.